Searching for potential ice-rich mining sites on the Moon with the Lunar Volatiles Scout

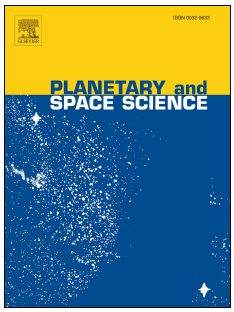

Searching for potential ice-rich mining sites on the Moon with the Lunar Volatiles Scout

J. Biswas, S. Sheridan, C. Pitcher, L. Richter, M. Reganaz, S.J. Barber, P. Reiss

PII: S0032-0633(19)30176-X

DOI: https://doi.org/10.1016/j.pss.2019.104826

Reference: PSS 104826

To appear in: *Planetary and Space Science*

Received Date: 30 April 2019

Revised Date: 28 November 2019

Accepted Date: 16 December 2019

Please cite this article as: Biswas, J., Sheridan, S., Pitcher, C., Richter, L., Reganaz, M., Barber, S.J., Reiss, P., Searching for potential ice-rich mining sites on the Moon with the Lunar Volatiles Scout, *Planetary and Space Science* (2020), doi: https://doi.org/10.1016/j.pss.2019.104826.

Author contributions

Manuscript title: Searching for potential ice-rich mining sites on the Moon with the Lunar Volatiles Scout

Author: Janos Biswas

Contributions: Conceptualization, Methodology, Investigation, Writing - Original Draft,

Author: Simon Sheridan

Contributions: Conceptualization, Methodology, Investigation, Writing - Review & Editing

Author: Craig Pitcher

Contributions: Methodology, Investigation

Author: Lutz Richter

Contributions: Conceptualization, Writing - Review & Editing, Supervision

Author: Mattia Reganaz

Contributions: Methodology, Investigation

Author: Simeon J. Barber

Contributions: Conceptualization, Writing - Review & Editing, Supervision

Author: Philipp Reiss

Contributions: Conceptualization, Methodology, Project administration, Writing - Review & Editing

Searching for potential ice-rich mining sites on the Moon with the Lunar Volatiles Scout

J. Biswas[a](j.biswas@tum.de), S. Sheridan[b], C. Pitcher[b], L. Richter[c], M. Reganaz[c], S. J. Barber[b], P. Reiss[d]

[a]*Institute of Astronautics, Technical University of Munich, Boltzmannstr 15, 85748 Garching, Germany*

[b]*School of Physical Sciences, The Open University, Milton Keynes, MK7 6AA, United Kingdom*

[c]*OHB System AG, Manfred-Fuchs-Straße 1, 82234 Weßling, Germany*

[d]*European Space Agency, ESTEC, Keplerlaan 1, 2201 AZ Noordwijk, The Netherlands*

Abstract

Multiple remote observations have indicated the existence of ice deposits in permanently shadowed regions (PSRs) near the lunar poles, nurturing hopes of possible future resource exploitation. However, the interpretation of the orbital data remains ambiguous and ground truth data is necessary for validation. The Lunar Volatiles Scout (LVS) is an integrated instrument for regolith sampling, gas extraction, and analysis that enables mobile prospecting for lunar volatiles, such as loosely adsorbed water and subsurface ice up to a depth of 10 cm. This study presents results of breadboarding activities using an integrated prototype of the LVS instrument to investigate soil insertion and to demonstrate gas extraction and analysis in thermal vacuum. The required vertical force for LVS insertion into dry and ice-bearing regolith was determined to be less than 15 N and sample-to-sample cross-contamination was found to be negligible. Thermal-vacuum test results proved the successful extraction of water from a hydrated lunar regolith simulant and detection of species across a mass to charge ratio m/z range of 15 to 200.

1 Introduction

The existence of water and other volatiles on the Moon has sparked great interest among researchers in the recent decade, both for its potential as a resource for future exploration missions and for what it could reveal about the mobility of volatiles within our solar system since its formation

(Anand, et al., 2014). Various missions, such as Clementine (Nozette, et al., 1996), Lunar Prospector (Feldman, et al., 1998), Cassini (Clark, 2009), Deep Impact (Sunshine, et al., 2009), Chandrayaan-1 (Pieters, et al., 2009), Lunar Reconnaissance Orbiter (Mitrofanov, et al., 2012), and LCROSS (Colaprete, et al., 2010) have investigated the existence of lunar water using neutron spectroscopy, visual, infrared and ultraviolet spectroscopy, and radiometry.

Infrared spectroscopy measurements indicate changes in surface regolith hydration during the lunar diurnal cycle (Clark, 2009) and an increased hydration towards higher latitudes (Pieters, et al., 2009). Indications of significant amounts of water ice in regions where the surface temperature never exceeds 110 K were found by ultraviolet spectroscopy (Hayne, et al., 2015). These were further confirmed by reflectance measurements (Fisher, et al., 2017) and infrared spectroscopy measurements (Li, et al., 2018). Neutron spectroscopy data suggest areas of enriched hydrogen abundance near the lunar poles, however the spatial resolution remains poor and the interpretation of the results remains ambiguous (Teodoro, et al., 2014). In 2009, the Lunar Crater Observation and Sensing Satellite (LCROSS) observed the ejecta of an artificial impact event in the permanently shadowed Cabeus crater, indicating a water ice content of 5.6 +/- 2.9% and significant amounts of hydrogen sulfide, ammonia, sulfur dioxide, carbon dioxide, various hydrocarbons and hydroxyl (Colaprete, et al., 2010). To date, this is the strongest evidence for the existence of significant amounts of water and other volatiles on the Moon, however further data on their physical state, nature, and spatial distribution is needed.

Simulations have provided further insight into the likely distribution of ice at the lunar poles. Paige et al (2010) have created a model that predicts the stability of ice in regolith as a function of depth and temperature, using surface temperature data obtained from the LRO Diviner Lunar Radiometer experiment. The results confirm that surface ice should survive within permanently shadowed regions (PSR) and that ice covered by a regolith layer of a thickness up to 10 cm should remain stable (sublimation rate below 1 kg/m^2 per billion years) at around 15 % of the surface area at the lunar South Pole (latitude < -80°).

Hurley et al (2012) presented Monte Carlo simulations of space weathering effects on ice deposits in PSRs. In their simulations, they subjected an initially solid layer of surface ice to millions of years of micro-meteorite bombardment. Over time, the layer breaks up and the pieces get buried, resulting in a heterogeneous volatiles distribution. In a similar study, Farrel et al (2015) investigated how space weathering effects can cause a spillage of volatiles from the floor of PSRs onto adjacent surfaces. As a result, they suggested that by measuring the volatiles content of the more accessible terrain surrounding a PSR the actual volatiles content within the PSR could be inferred.

In light of these findings, the next logical step for the exploration of lunar volatiles will be surface missions to provide ground truth data in multiple selected regions. In 2014, the Lunar Exploration Analysis Group (LEAG) formed the Volatiles Special Action Team (VSAT) that defined five priority measurements for future landed missions (Bussey, et al., 2014), which were further endorsed by the Topical Team on Exploitation of Local Planetary Materials of the European Space Agency (ESA) (Anand, et al., 2015):

1. Variability of volatiles distribution (lateral and vertical)
2. Chemical phase of volatile elements
3. Chemical and physical behavior of polar soil with temperature
4. Geotechnical properties
5. Current volatile flux

The LEAG report identifies a rover with subsurface sampling capability as the most suitable approach to obtain these measurements. The authors highlight two regions near the lunar South Pole (in the vicinity of the Cabeus crater and the Shoemaker/Nobile crater) and one region near the North Pole (in the vicinity of the Peary crater) as ideal landing sites. All three regions contain multiple sites that provide some solar illumination for the operation of solar powered systems and Earth visibility for communication. They also lie close to a PSR (<1 km), are sufficiently level for rover operations (slopes <10°) and show increased hydrogen concentrations from orbital neutron spectroscopy measurements (Bussey, et al., 2014).

To enable future volatiles exploration missions, instrumentation is needed for the investigation of volatiles that complies with the strict mass, power and volume constraints of lunar rovers. This paper presents the Lunar Volatiles Scout (LVS), an integrated soil sampling and analysis instrument for lunar in-situ measurements that is designed to be carried by a small rover. Specifications and detailed design of the instrument are presented as well as preliminary instrument characterization results from laboratory tests.

2 Scientific Objectives

The main purpose of the LVS is to address the first of the aforementioned LEAG VSAT priority measurements: Determine the lateral variability of volatiles distribution on the lunar surface. Thus, it needs the abilities to sample lunar soil at different depths down to at least 10 cm, determine the chemical species of volatiles in the sample, their relative concentrations, and ideally their abundance. Additionally, the LVS offers the opportunity to address some of the other priority measurements. Outgassing rates as a function of temperature can provide indications on the chemical phase of the released volatiles. Geotechnical properties, such as bulk density, cohesion, and internal friction angle may be inferred from the force required to insert the LVS into the ground. Finally, volatiles may also be released from the regolith by mechanical interaction of the rover wheels with the soil or by heating of the soil due to the rover's presence or changing solar illumination. Continuous measurement of these volatiles during the rover traverse can provide further insight into the dynamics of volatiles on the lunar surface or indicate locations of interest for sampling. In summary, the LVS shall:

- Extract and analyze volatiles from lunar regolith
- Measure the insertion force as a function of depth
- Measure free volatiles released from the regolith by rover wheels or solar illumination

Figure 1 shows a sketched reference mission scenario for the LVS in which a lunar lander touches down in the polar region and a small rover carrying the LVS is deployed. Multiple investigations can be performed in this scenario as described in the following.

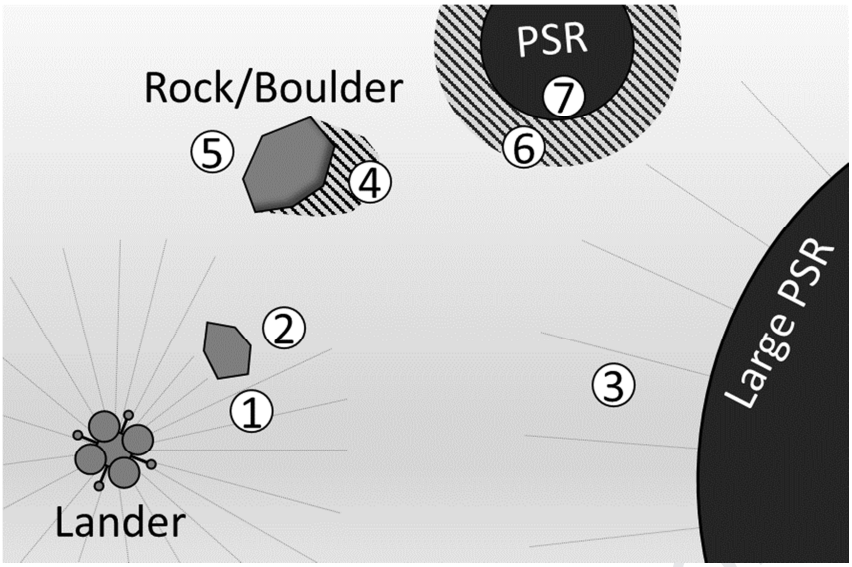

Figure 1: Sketched top down view of an example landing site for the LVS with highlighted sites of interest: (1-2) Landing site contamination assessment; (3) Search for volatile enriched locations due to spillage in vicinity of large PSR; (4-5) Investigation of locally shadowed (low-temperature) –as well as illuminated (high-temperature) areas around a boulder; (6-7) Investigation of a small, accessible PSR and its surrounding temporary shadow.

After rover deployment and commissioning, the LVS takes multiple samples in the vicinity of the lander to assess the extent of surface contamination by the retro-propulsive rockets (1) and possible shielding effects by rocks or boulders (2). Measuring the potential contamination is not directly relevant to the science objectives, but it provides useful context for the measurement of volatiles by static landers, such as Luna-27 with the ESA PROSPECT payload (Trautner, et al., 2018). In addition, these measurements establish a baseline and demonstrate system functionality in the relative safety close to the lander. The second target is the vicinity of a large PSR (3), where multiple investigations are performed at different distances to verify model predictions about increasing concentration of volatiles towards the PSR (Farrel, et al., 2015). The third target is the investigation of volatiles in different illumination conditions. Orbital observations indicate diurnal changes in surface volatiles concentrations with an increase in cold shadow and a decrease in hot illuminated areas (Clark, 2009). The low solar elevation in the lunar polar regions in combination with its long diurnal cycle of 28 days means that even small boulders can cast large, long-lasting shadows in which the regolith will cool down significantly, while the illuminated side of a boulder and the regolith directly in front of it

will get very hot due to direct solar illumination, albedo, and infrared radiation from the boulder. Thus, the LVS would perform investigations both in shadow (4) and in front of the boulder (5) to have a direct comparison. Finally, the rover would investigate a small, accessible PSR, performing multiple measurements with the LVS in the PSR vicinity (6) and directly inside (7).

It should be noted that this reference scenario is an ideal case. An actual mission scenario will be subject to various constraints and may include conflicting schedule demands from other payloads and will therefore exclude certain measurements. A more detailed mission scenario for the LVS is currently under investigation as part of the "Lunar Volatiles Mobile Instrumentation - extended" (LUVMI-X) study. The LUVMI-X rover has a mass of 40 kg, the ability to enter and operate within small accessible PSR's, and includes various other payloads. It is solar-powered and capable of operating for at least 14 days (Gancet, et al., 2017) (Gancet, et al., 2019).

3 Instrument Description

The LVS presents an innovative approach to lunar volatiles prospecting, by performing sample acquisition, heating, and analysis directly in-situ in the ground and thus avoiding complex sample handling and preparation mechanisms. This is illustrated in Figure 2: The LVS consists of an augered drill shell with a central heating element that can be inserted into the ground. Once inserted, the heating rod heats the enclosed sample and the volatiles are released and detected by an ion-trap mass spectrometer (ITMS) directly above the drill shell. The concept, which was originally developed through the LUISE activity funded by the German Aerospace Center DLR (Reiss, et al., 2015), is similar to the "Sniffer" concept for volatiles extraction presented by Zacny et al (2016) as part of the Planetary Volatiles Extraction (PVEx) study, but implemented in a simpler fashion.

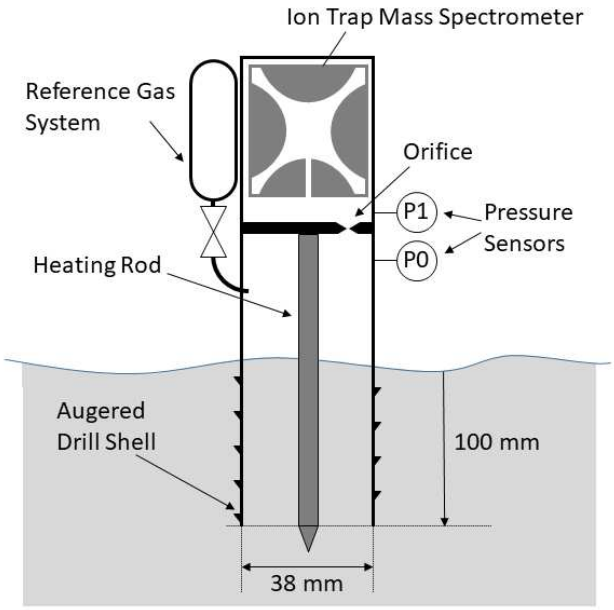

143

144 *Figure 2: Schematic of the LVS*

145 For the present study with the LVS prototype, heating was conducted with 15 W constant power for
146 a time of 90 min in high vacuum. The resulting temperatures depend strongly on the insertion depth
147 and water content. For 10 cm insertion depth with completely dry regolith and 90 min of heating, the
148 maximum achievable temperature is around 500 °C. This is sufficient to sublimate water ice (Feistel,
149 et al., 2007) and release loosely adsorbed water (Poston, et al., 2013), but may not be enough to
150 release chemically bound volatiles. Higher temperatures could be achieved by a longer heating
151 duration or reduced sample size, but this has not been investigated further so far.

152 After release, volatiles either remain trapped within the drill shell, move towards the ITMS through a
153 small orifice, or escape downwards through the regolith. A preliminary study showed that 44 % of
154 the released gas was lost this way in a comparable setup (Parzinger, et al., 2013), though this also
155 depends on regolith properties, temperatures, and achieved gas pressures in the shell.

156 Above the shell, the ITMS is mounted, which analyses the chemical species in the evolved gas. The
157 ITMS volume is connected to the sample volume via a small orifice to ensure that the pressure in the
158 ITMS volume does not exceed the operational limit of 10^{-3} mbar. Pressures inside both the sample
159 volume and the ITMS volume are recorded by Pirani pressure sensors, which cover a range of

10^{-3} mbar to 10 mbar. The pressure inside the sample volume may be used as an indication for the abundance of volatiles or the diffusivity of the sample (Reiss, 2018). The ITMS itself is a single unit comprising the Quadrupole Ion Trap Mass Spectrometer (March, et al., 2005) and associated control electronics (see Figure 3). The ITMS draws on heritage of the Ptolemy ITMS instrument which made the first in-situ measurements of volatiles and organics on comet 67P on board the Rosetta lander Philae in 2014 (Morse, et al., 2015) (Wright, et al., 2015). In the ITMS released gases are ionized by a filament electron source. The ions are then stored in the electrode cavity by a radio frequency (RF) trapping field that is applied to the ring electrode of the ITMS. The RF amplitude is increased and as the voltage exceeds a threshold, the ions within the ion trap are ejected onto an electron multiplier for detection. The voltage at which the ions are ejected from the trap is given by:

$$v_{ej} = \frac{m r_0^2 \Omega^2}{4e}$$

Where m is the mass of the ion, r_0 is the inner radius of the ring electrode, e is the electron charge and Ω is the RF angular frequency. The ion trap has r_0=8 mm radius, and operates with a frequency of 550 kHz, giving an ejection voltage of around 2 V per mass unit. The RF field was generated from a 12 bit control voltage using a tuned resonance LC circuit (inductor (L) and capacitor (C) wired in parallel) capable of producing a maximum voltage of about 800 V peak-to-peak on the ring electrode. A software programmable scan function was used to control the voltages on the ion trap electrodes with a typical scan function shown in Figure 4.

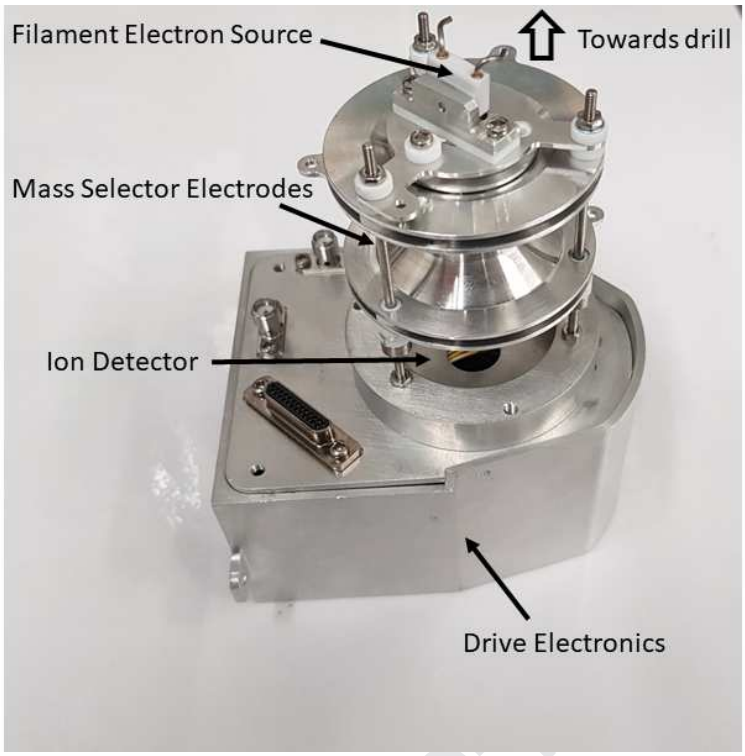

177

178 *Figure 3: Image of the LVS ITMS prototype.*

179

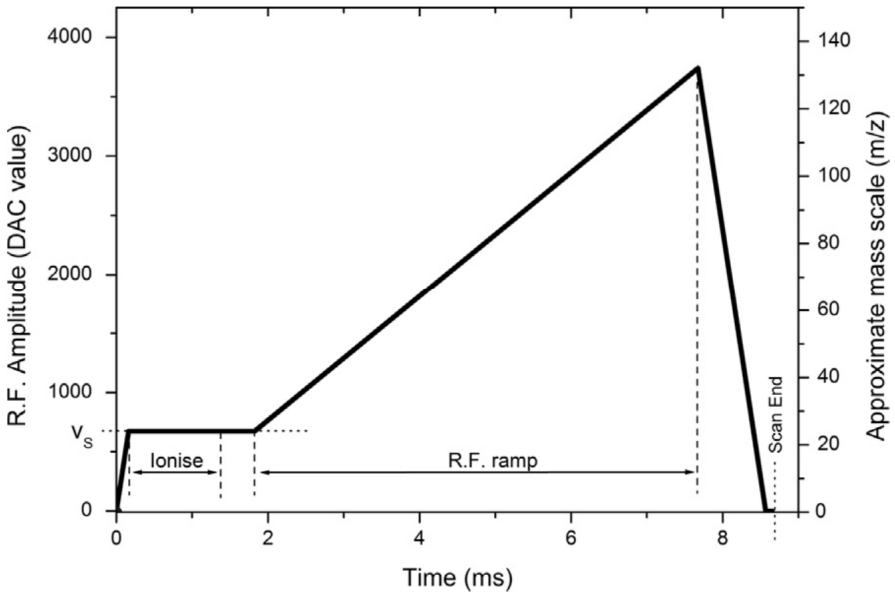

180

181 *Figure 4: A typical ion trap scan function: Electrons are admitted into the ion trap cavity whilst the radiofrequency (RF)*

182 *voltage (amplitude of the RF voltage) is held at the storage voltage (V_S). Following ionization and after allowing 0.5 ms for*

183 *trapped ions to settle, the RF voltage is ramped to eject ions from the trap in order of ion mass. Unit of the RF voltage is*

184 *reading of the 12 bit digital to analog converter (DAC).*

This device offers a mechanically simple, low mass, volumetrically compact mass spectrometer that can be used to perform rapid identification and characterization of volatiles in real time as they are delivered to the instrument. In operation the gas inside the ITMS must not exceed a certain pressure to protect the filament electron source, which is ensured by the dimensioning of a vent orifice to the lunar exosphere. The operational mass range of the ITMS will allow a wide range of species to be detected and characterized.

Table 1: Instrument specifications of the LVS (values of the prototype)

Total mass:	1.9 kg
Power:	< 20 W
Mass spectrometer range:	m/z 15 to 200
Mass resolution:	2
ITMS lower detection limit:	$1x10^{-10}$ mbar
ITMS max operating pressure	$1x10^{-3}$ mbar

An image of the latest LVS prototype is shown in Figure 5 and the main properties are summarized in Table 1. Its augered drill shell has a length of 150 mm and an inner diameter of 38 mm, enclosing a maximum sample volume of 163 cm^3 and resulting sample masses between 245 g and 277 g, for bulk densities between 1.5 g/ cm^3 and 1.7 g/cm^3. The shell can be rotated by a brushed DC motor for eased insertion. On top of the drill, the pressure sensors, the ITMS, and a reference gas system is mounted. The reference gas system will allow the injection of small quantities of a compound with a known mass spectrum, such as perfluorotributylamine (PFTBA) for on-board recalibration of the ITMS to account for possible contaminants from prior samples or outgassing of rover components.

The entire LVS instrument fits into a 120 mm x 120 mm x 400 mm envelope and has a total mass of 1.9 kg. The Power consumption of the LVS during insertion and heating is below 20 W.

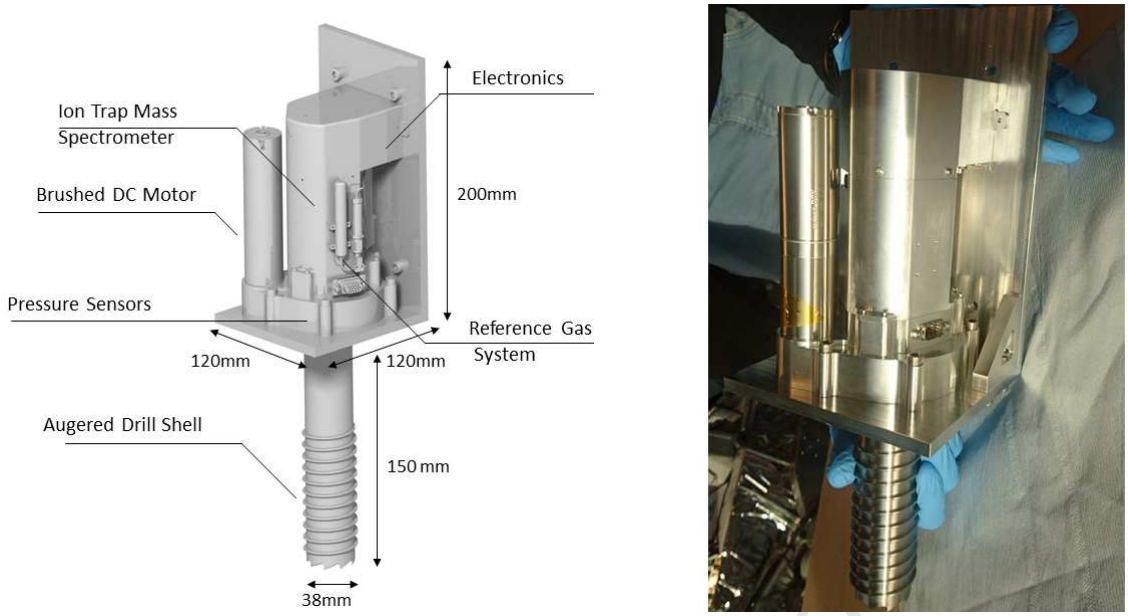

204

205 *Figure 5: Left: render image of the LVS including dimensions and annotations, Right: Actual image of the prototype.*

206 # 4 Instrument Characterization

207 The instrument characterization was performed in four steps: (1) investigate the mechanical
208 insertion of the LVS into lunar regolith simulant, (2) characterize ITMS performance, (3) characterize
209 the LVS drill and heater in thermal vacuum environment, and (4) test the LVS integrated with the
210 ITMS. Based upon the knowledge gained through previous proof of concept tests of different
211 subsystems, a special test facility was set up to enable the increasingly complex activities to achieve a
212 full instrument characterization in a relevant environment. Each of the four separate goals of the
213 characterization campaign is described in more detail in the following sections. ITMS tests were
214 performed at the facilities of the Open University, while the mechanical, gas extraction and
215 integrated prototype tests were performed at the Technical University of Munich.

216 ## 4.1 Mechanical Insertion

217 The purpose of this test was to predict the ability of the LVS to sample lunar soil with different ice
218 contents. This included observing the behavior of the ice-bearing sample, estimating sample cross-
219 contamination, and determining the penetration force. The latter is of particular relevance for small
220 rovers because they can only provide a limited vertical force under lunar gravity (for example a 20 kg
221 rover can only provide a maximum vertical force of 32 N at 1.6 m/s²).

For the purposes of this study, the lunar surface was approximated using the JSC-1A lunar regolith simulant (Zeng, et al., 2010) contained in a 10 l bucket. The simulant was prepared by loosening with a rake, mixing with the desired amount of water while stirring until the water was homogenously distributed, and subsequent freezing with liquid nitrogen. Hydrated samples yielded average bulk densities of 1.44 g/cm^3 for 2.5 wt% water and 1.48 g/cm^3 for 5.0 wt% water (Table 2). The prepared dry simulant achieved an average bulk density of 1.68 g/cm^3, which corresponds to a friction angle of 40° ±2° (Iai, et al., 2011). According to Zeng et al (2010) JSC-1A has negligible cohesion. Lunar regolith at the Apollo landing sites has an average bulk density of 1.58 ±0.05 g/cm^3, an average friction angle of 44° - 47°, and an average cohesion of 0.9 kPa for a depth up to 30 cm (Carrier, et al., 1991). Because the shear strength and the bulk density are lower under lunar gravity we consider these test conditions as sufficiently conservative. Hydrated samples yielded lower bulk densities, but no data is available yet from actual icy lunar samples for comparison.

Table 2: Insertion test conditions and results

Test case	Water content [wt%]	Soil temperature [°C]	Average bulk density [g/cm³]	Average soil residuum [g]	Average force at 10 cm [N]
A	0.0	Ambient	1.68	0.026	12.4
B	2.5	-156	1.44	0.040	8.7
C	5.0	-158	1.48	0.034	11.1

For the initial drill tests the drill was activated and moved downwards into the simulant at constant speed while the force was recorded via a load cell. An important parameter for the insertion is the speed ratio, which is the ratio of rotational versus vertical speed of the drill shell. A higher speed ratio allows a lower penetration force but also causes higher mechanical sample disturbance. The speed ratio was chosen such that the vertical haulage of the drill auger is twice as high as the vertical insertion speed, as this was found to be an optimum between low sample disturbance and low penetration force.

Three sets of test cases with six individual tests each were conducted: test case A with dry JSC-1A at ambient conditions and test cases B and C with 2.5 % and 5 % water mass content at temperatures below -150 °C, which corresponds to temperature estimates for stable water in PSRs (Colaprete, et al., 2010) (Hayne, et al., 2015). The resulting forces over depth are shown in Figure 6: For all cases, the penetration force rises moderately to less than 15 N at 10 cm depth and then starts to rise sharply. No significant difference in vertical force was observed between icy or dry samples. A possible explanation for the sharp increase below 10 cm could be that the auger on the drill shell does not extend all the way up the shell and may lose effectiveness when it is fully inserted in regolith. Another explanation is the strongly increasing bulk density and shear strength at greater depths in the soil.

To assess possible sample-to-sample cross-contamination, the soil residuum on the instrument was measured. For the retraction the drill was rotated in the reverse direction, which expelled the majority of the sample from the drill shell. After each test the instrument was visually inspected and then dismantled. The mass of soil residuum on the drill shell, which essentially was dust sticking to the surfaces, was determined on a scale. In all cases, the residuum mass was less than 0.25 % of the average dry sample mass. The sample masses for the insertion depth of 100 mm ranged between 157 g and 183 g.

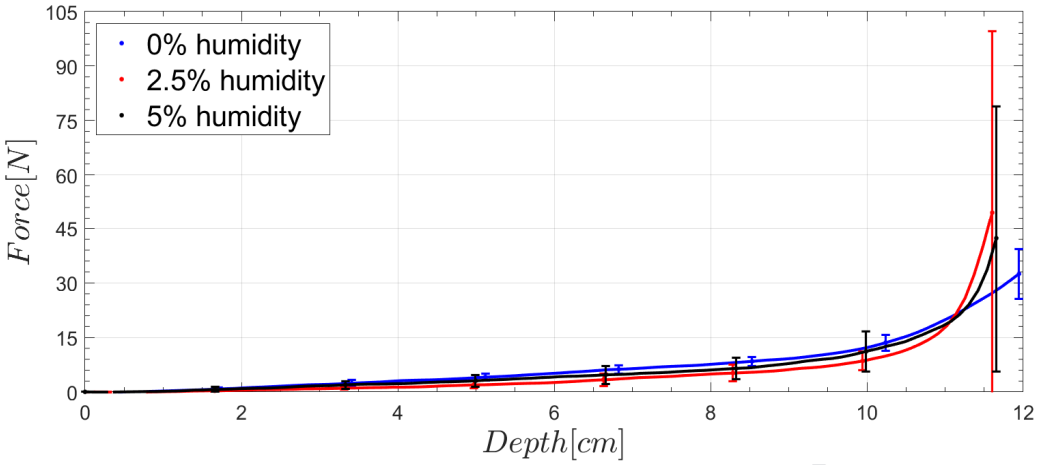

Figure 6: Average penetration force over depth for the LVS in JSC-1A lunar regolith simulant with six individual tests per test case. Error bars indicate the one sigma standard deviation at arbitrary intervals on the curves.

4.2 Characterization of the ITMS

The purpose of this test was to verify the capability of the ITMS to identify chemical species across the specified mass range. For this purpose the ITMS was placed in a vacuum chamber, into which a flow of PFTBA was admitted. PFTBA is a compound that is frequently used for mass spectrometer calibration because it yields a range of characteristic fragments with known mass to charge ratio (Creaser, et al., 200). Figure 7 shows the acquired mass spectrum together with the RF voltages of the PFTBA peaks. The peaks confirm the expected linear relationship between m/z and ejection voltage. Using this correlation, the ejection voltage of the RF field can be used to determine the m/z values of the chemical species that are released by the LVS. The results also show that m/z values between 15 and 219 can be identified.

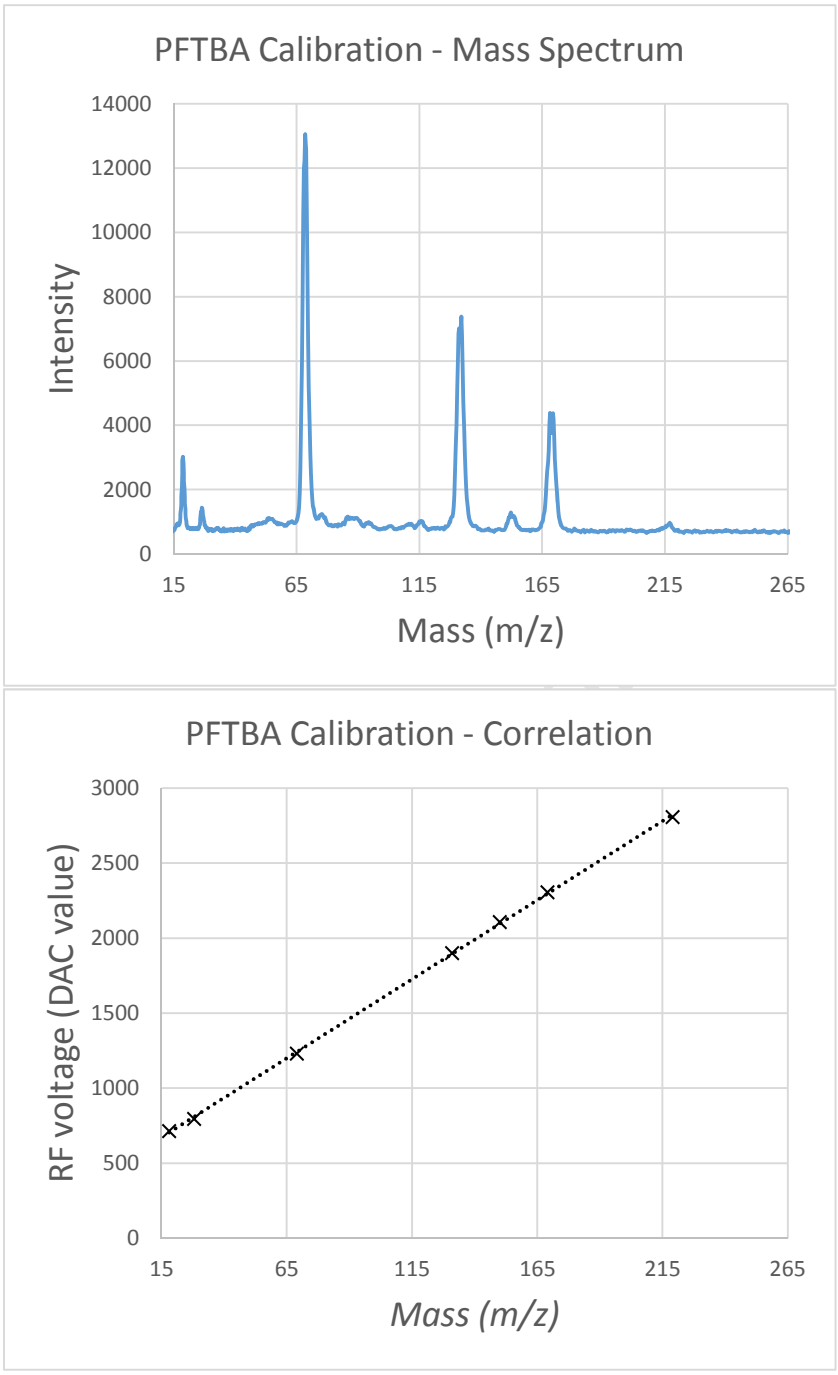

Figure 7: Results of the ITMS from calibration with perfluorotributylamine (PFTBA). Upper panel: Full mass spectrum after PFTBA injection. Lower panel: RF field amplitude digital to DAC reading over m/z ratio. Crosses indicate (known) peaks in the PFTBA spectrum.

4.3 Characterization of Gas Extraction

The purpose of this set of tests was to demonstrate the ability of the LVS to extract volatiles from icy regolith samples and to characterize the relation between the abundance of volatiles and gas pressures generated by their release. A schematic of the test setup is shown in Figure 8. The tests were conducted in a thermal vacuum setup that consists of a vertical actuator above a sample

container. The sample container is enclosed by a cold shroud, which can be cooled by liquid nitrogen. The chamber uses a dust-tolerant Leybold T350i turbo-molecular pump and the pressure is monitored by a Leybold Penningvac PTR 90 sensor, which also serves to calibrate the Pirani sensors of the LVS. The sample temperature is measured by a 0.5 mm metal sheath thermocouple, which is inserted to a depth of 5 cm at a distance of about 3 cm to the inserted drill shell. In addition, a webcam provides a live video feed from inside the vacuum chamber.

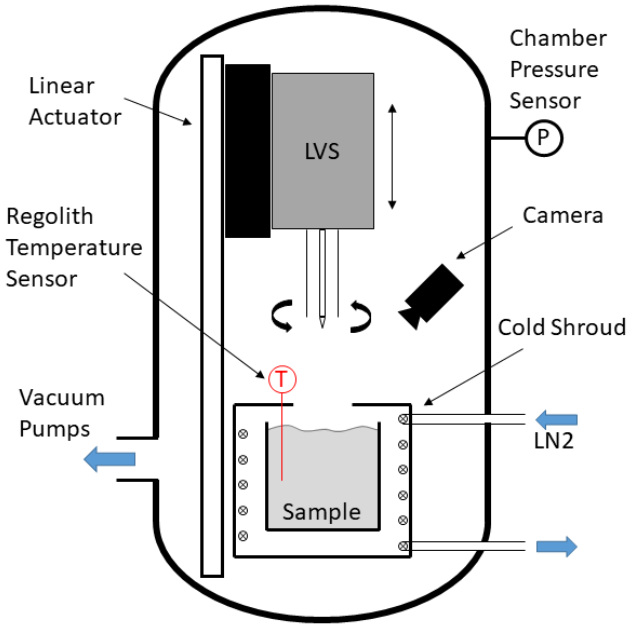

Figure 8: Schematic of the thermal-vacuum test setup.

Pictures of both the LVS in the chamber and a prepared sample are given in Figure 9. For this set of tests the ITMS was not attached. Samples were prepared analogously to the insertion experiments, but were frozen under ambient pressure to -50 °C before the chamber was evacuated. Noticeable loss of volatiles from the cooled sample container due to vacuum alone was observed only in the topmost 1 – 2 cm during evacuation of the vacuum chamber. The test procedure is detailed in Table 3.

Table 3: Operational procedure for the gas extraction tests

Step	Time [hh:mm]	Description	Duration
1.	T -24:00	**Sample preparation**: Samples are prepared (and hydrated for icy	-

		samples) and mounted in vacuum chamber.	
2.	T -18:00	**Freezing**: Hydrated samples are frozen to -50°C.	-
3.	T -06:00	**Evacuation:** The chamber is evacuated to below 10^{-4} mbar.	-
4.	T -03:00	**Bakeout**: After evacuation and prior to sampling, the LVS heater is activated at 15 W for 30 min to bake out moisture and other contamination from the heater and the drill shell.	30 min
5.	T +00:00	**Drilling:** The drill is activated and lowered by the linear guide for insertion into the sample until the desired depth is reached.	5 min
6.	T +00:10	**Heating**: The heating rod is activated with a constant power of 15 W.	90 min
7.	T +01:50	**Retraction:** The drill is activated and raised by the linear guide until it is completely retracted from the sample.	5 min
8.	T: +02:00	**End of test**.	-

Figure 9: Left: Image of the LVS on the vertical actuator inside the thermal vacuum test setup. Right: Image of a hydrated frozen JSC-1A sample in the sample container.

The purpose of the first test was to verify the test setup and the sample preparation procedure. For the subsequent tests to be meaningful, the setup and procedure must yield reproducible results. Thus, three dry samples were prepared at room temperature. Due to the preparation in ambient air, the actual water mass contents ranged from 0.09 % to 0.12 % by weight. Outgassing tests were performed on each of these samples, using a test procedure that was identical in all three cases, except for a small drop in heating power during the first test due to a software failure. Nonetheless, Figure 10 shows that the evolution of the gas pressure inside the drill shell is very similar for all three cases. The pressure starts to rise after about 4 min, which corresponds to the time of first contact between the drill shell and the sample. This increase in pressure can be attributed to mechanical disturbance of the sample surface. Thermal release can be ruled out, since the sample was not cooled for this test and had the same temperature as the drill. The pressure slowly rises further during drilling up to 10 min into the test when the heating was initiated. Here a significantly steeper pressure rise is visible and a maximum of approximately 1 mbar is reached after about 80 min of heating. The comparison of these three test runs with dry simulant proves that the setup and especially the sample preparation procedure generate reproducible results. Furthermore, in all three tests the heater temperature curve reaches a maximum value after about 50 min of heating after which the temperature falls again, even though the heating was not interrupted. The reason for this effect is that the thermal conductivity of the regolith increases with pressure and temperature (Reiss, 2018), therefore the heater temperature decreases.

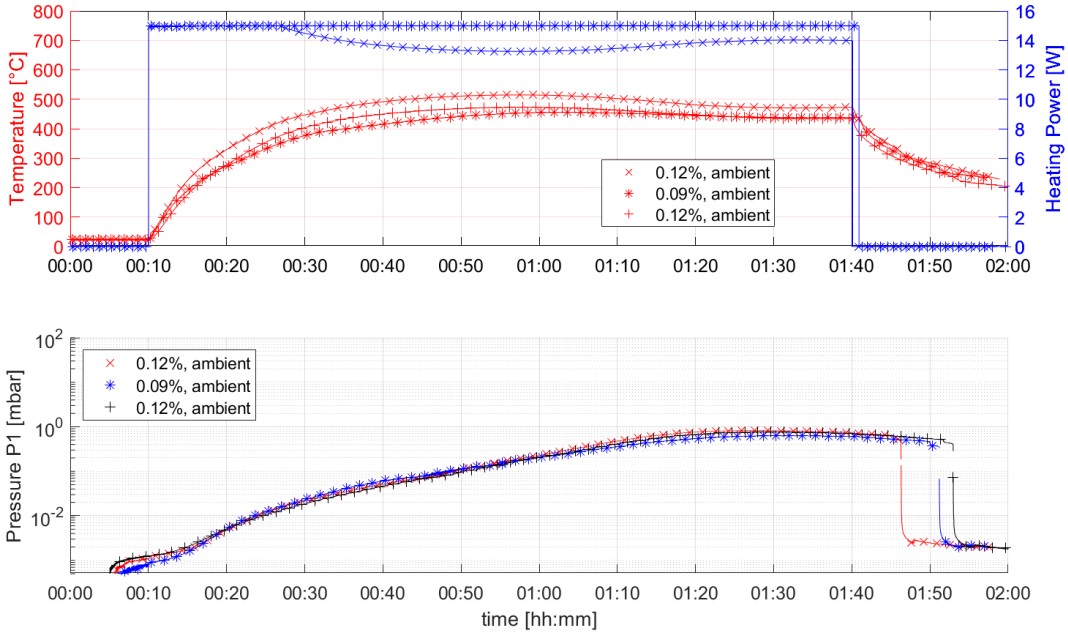

322

323 *Figure 10:* Gas extraction results for three tests at ambient temperatures and 0.09 % - 0.12% water mass content. Time
324 scale corresponds to operational procedure.

325 The second test series aimed at showing the pressure evolution for different water contents of the
326 sample. Five different samples were prepared, with water mass contents between 0.6 % and 5.3 %.
327 The samples were frozen and held between -50 °C and -60 °C during evacuation. The results are
328 shown in Figure 11. Similar to the previous test series, the pressures starts to rise immediately after
329 the drill makes contact with the soil at 4 min. For the 0.6 % case the pressure rises to 0.01 mbar
330 almost immediately and rises more slowly until it reaches sensor saturation at 10 mbar about 40 min
331 after initial contact (corresponding to about 35 min after heating was started). The initial pressure
332 rise is higher and sensor saturation is reached sooner with higher water contents, with the exception
333 of the 5.3 % curve, which lies slightly below the 3.9 % curve.

334 All curves reach a maximum at about 10 mbar, since this is the upper measurement limit of the Pirani
335 pressure sensor. As with the previous tests the heater temperatures reach a maximum and then start
336 to drop again. However, towards the end of the tests the heater temperatures rise again, because
337 the pressures start to fall. The maximum temperatures in the sample were significantly lower than in
338 the previous test series. This is expected, because releasing the higher amount of volatiles requires
339 more latent heat and the higher resulting pressures increase the thermal conductivity. It is

noteworthy that the heater temperature at the beginning of the test was not identical for all cases. Due to minor differences in the procedure, the initial temperature of the heating element was about 40 °C higher in the cases of the 0.6 % and 1.6 % samples. However, the pressure response from these two samples was the slowest despite this increased initial temperature.

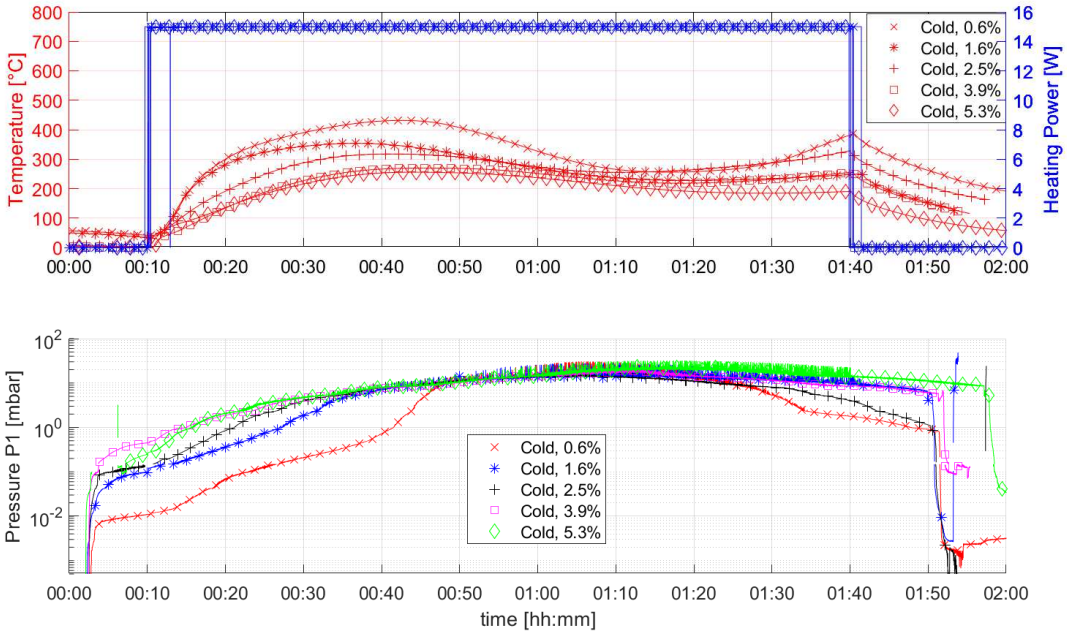

Figure 11: Gas extraction results for samples with different water mass contents. Time scale corresponds to operational procedure.

4.4 Combined gas Extraction and Analysis

The purpose of this final test was to demonstrate that the LVS can extract volatiles from a regolith sample and identify the present chemical species. For this test a sample with 0.2 % water mass content was prepared and evacuated at ambient temperatures. The test procedure was identical to the previous tests for evacuation. However, the heating was stopped after 5 min and the LVS was retracted from the sample. This was done to protect the ITMS, since its filament is sensitive to higher pressures, and it was unclear at the time if the system dimensioning would allow a continuous operation. However, as no issues were observed, the LVS was reinserted after 15 min and a full heating sequence of 90 min was performed. Figure 12 shows the heating power and LVS drill depth in

addition to the resulting pressure curves. Note that the Pirani sensors are unable to provide a signal at pressures below 10^{-4} mbar.

The ITMS was successfully operated during the entirety of the test, despite a pressure rise in the ITMS volume to $2 \cdot 10^{-3}$ mbar. Figure 13 shows three mass spectra that were acquired at different times of the test cycle. In all three plots clear peaks are visible at m/z 18 with a lower response at m/z 17 and 16, which is a very clear indication for the presence of water (Wallace, et al., 2018).

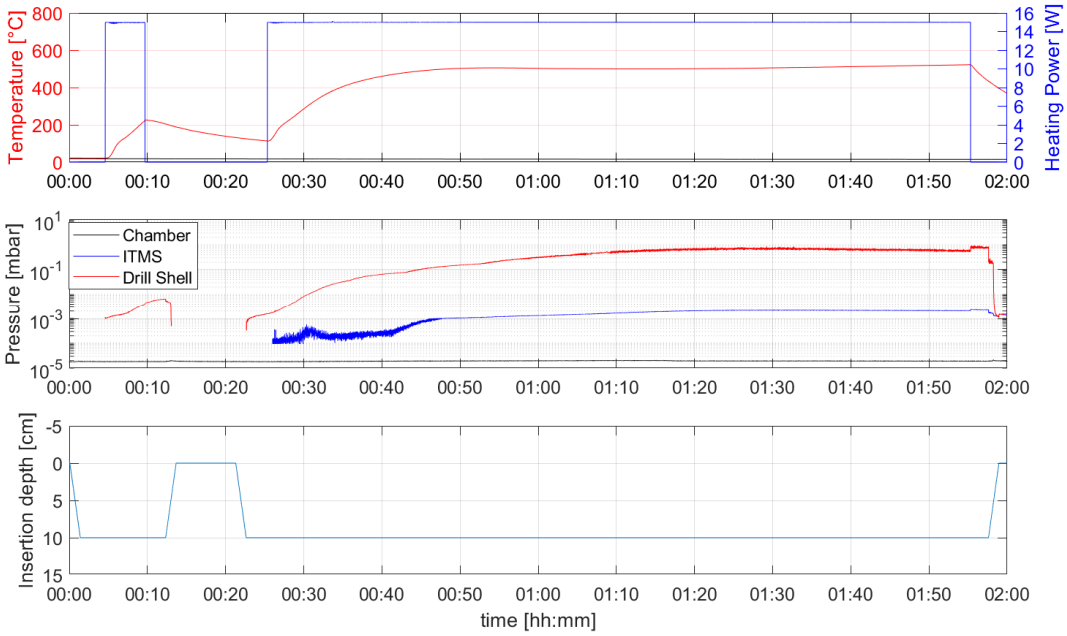

Figure 12: Gas extraction plots for the combined extraction and analysis test. Time scale corresponds to operational procedure.

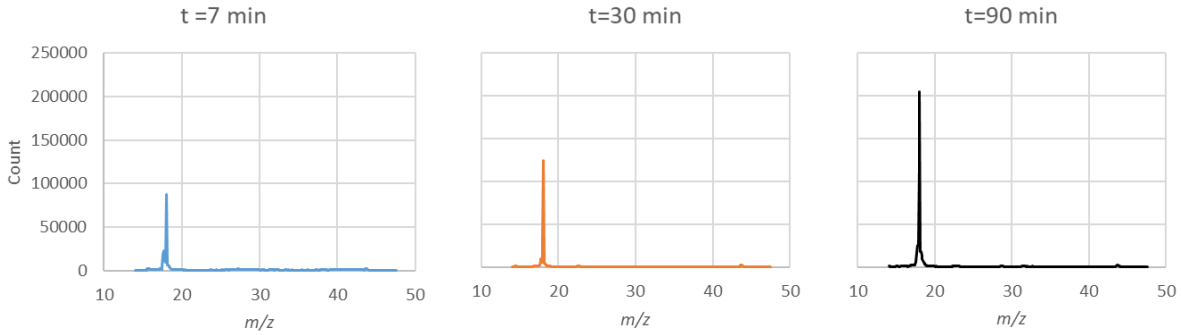

Figure 13: Mass spectra acquired by the ITMS at different times during the combined gas extraction and analysis testing

5 Discussion

The presented mechanical insertion tests showed that the LVS drill and operational concept allow insertion up to a depth of 10 cm, without exceeding the vertical force available on a typical small lunar rover. No significant strengthening of the lunar regolith by the presence of water ice was observed up to this depth. Atkinson and Zacny (2018) investigated the mechanical properties of hydrated frozen JSC-1A regolith simulant with bulk densities of 1.5 – 1.67 g/cm^3 and found that the unconfined compressive strength of the material increases with water content. However, the effect is less pronounced for lower bulk densities. The applied sample preparation procedure for this study did not involve deliberate soil compaction, resulting in fairly low bulk densities. While it is reasonable to assume that the topmost 10 cm of regolith on the Moon have a fairly low bulk density, further development of the LVS should also take higher densities into account.

The results also showed that the current LVS design is not suited to achieve greater depths. While water ice is predicted to remain stable at 10 cm depth in certain non-permanently shadowed regions (Paige, et al., 2010), these areas are challenging with respect to their thermal environment and may not provide sufficient illumination for rover and lander operations. Future development of the LVS should therefore include careful landing site selection and mission planning, and possibly investigate if a greater drill depth is achievable since it may allow to sample in more benign illumination and thermal conditions.

Testing of the ITMS with a calibration compound showed that the system can detect compounds with m/z between 15 and 219. This enables the detection of all of the chemical species detected in the LCROSS impact event (Colaprete, et al., 2010), though it is questionable if it will be possible to distinguish all individual compounds if they are all present at the same time. While it will be straightforward to distinguish the larger compounds like hydrogen sulfide, sulfur dioxide, or carbon dioxide, smaller molecules like water, ammonia, methane, and hydroxyl have similar fragmentation patterns (Wallace, et al., 2018) and determining each of the relative concentrations will be challenging. This issue needs to be investigated further, especially since the LCROSS data indicates

large differences in relative concentrations (e.g. the methane concentration relative to water was reported to be only 0.65 %).

The presented gas extraction results clearly show successful release and detection of water from the regolith simulant. The achieved maximum sample temperatures in the tests with low water content were in the range of 500 °C, which is comparable with the temperatures of the Resource Prospector payload OVEN that utilizes an extraction temperature of 450 °C (Kleinhenz, et al., 2018) for a similar purpose. However, further away from the heating rod the regolith temperature was likely much lower and a large temperature gradient inside the sample needs to be expected. This will become problematic if multiple species of volatiles with different outgassing temperatures are present in the sample. It needs to be investigated if the LVS will be able to determine the relative concentrations of the different species in this context. A simple solution could be to heat the sample to specific temperatures in steps and wait until the sample is sufficiently isothermal, though this will consume more time and energy. Operational constraints of the rover therefore mainly determine the feasibility of such operational modes of the instrument. It may also be beneficial to reduce the sample volume for future versions of the LVS to reduce the temperature gradients as well as the required heating power and duration. To investigate the multi-species measurement performance, it is currently envisioned to mix hydrated JSC-1A with calcium oxalate to create samples that contain multiple volatiles species for further testing with the prototype. Calcium oxalate releases chemically bound water at temperatures between 100 °C and 200 °C and carbon monoxide and carbon dioxide at about 500 °C and 800 °C respectively (Robertson, 2016).

The results shown in Figure 11 indicate that for multiple samples with different contents of the same volatiles species, the pressure tends to rise faster for higher volatiles contents. Though only large differences seem distinguishable, these may be used to gain limited insight into the abundances of volatiles by relative comparison of pressure responses at different sampling sites. It may also be possible to estimate the order of magnitude of the abundance of volatiles by careful comparison with ground calibration data. This subject needs further investigation in the frame of a more thorough

characterization study. Most importantly, the instrument can determine if and which volatiles are present at a particular location. Given the significant technical challenges and cost involved in landing instrumentation on the lunar surface, the LVS nevertheless provides a good compromise between measurement sophistication, mobility and cost, especially in the harsh environment of the lunar poles.

For comparison ESA's PROSPECT instrument package for the Luna-27 lander (Carpenter, et al., 2017) (Trautner, et al., 2018), which is built upon heritage of the Ptolemy instrument (Wright, et al., 2015), includes a drill, complex mechanisms, several single use sample ovens, and two mass spectrometers for the analysis of volatiles. PROSPECT accesses samples from greater depths (>1 m) and performs more detailed analyses at higher temperatures, including precise isotopic measurements and ISRU demonstrations (Barber, et al., 2018). However, the challenges of extracting and processing these samples whilst controlling sample alteration and potential loss of volatiles prior to sample analysis result in a complex mechanical system with a consequent total mass of 35 kg and 180 W peak power requirement and is therefore incompatible with a smaller rover. The expected heterogeneity in volatiles distribution due to impact gardening (Hurley, et al., 2012) means that abundances determined by PROSPECT on the static Luna-27 lander may not be representative for the wider surrounding area, and the lander's retro-propulsive rockets also bear the risk of landing site contamination.

An instrument package similar to PROSPECT has been developed by NASA for the Resource Prospector, a solar powered lunar rover designed for exploration of the lunar South Pole. With a payload capacity of 90 kg, it was intended to carry the TRIDENT drill, the Oxygen and Volatile Extraction Node (OVEN), the Lunar Advanced Volatile Analysis (LAVA), the Neutron Spectrometer System (NSS) and the Near Infrared Volatiles Spectrometer System (NIRVSS) to prospect for volatiles in and around PSRs and down to a depth of 70 cm (Andrews, et al., 2015). Resource Prospector was cancelled, but some of its instrumentation may be reused in the new Volatiles Investigating Polar Exploration Rover (VIPER) program.

The LVS, in contrast, is a volatiles prospecting instrument, designed to be carried by a small rover (>10 kg) and as such it respects strict constraints regarding mass, volume, power consumption and sampling time. This makes it compatible with various landers and rovers, like LUVMI-X (Gancet, et al., 2019) or Polar Ice Explorer (Calzada-Diaz, et al., 2018). As discussed here, it can provide limited information about the physical state, chemical composition, and lateral variability of lunar volatiles, which make it an ideal inexpensive precursor scouting instrument to a more complex mission, or a suitable mobile complement to a non-mobile instrument like PROSPECT.

An additional goal of the LVS was to capture free volatiles from the lunar environment, which are released from the regolith by rover motion or changing illumination conditions. This was not investigated in the presented tests. Generated gas pressures are likely to be extremely low, which is complex to simulate in a laboratory setup. However, the LVS ITMS builds upon the Ptolemy instrument of the Rosetta Philea lander. Despite the unfortunate landing of Philea, Ptolemy was able to generate useful data from the gases that were released when Philea touched down on Comet 67P/Churyumov-Gerasimenko (Morse, et al., 2015). Touching down at multiple sites, Ptolemy was able to identify differences in the chemical compositions of the comets coma at different landing sites, indicating a heterogeneity of the comets nucleus. Running the LVS ITMS in a background sniffing mode while the rover traverses the lunar polar landscape is likely to provide similar results, possibly identifying interesting sites for further investigation.

6 Conclusion

The main objective of the LVS development was to provide a tool to address the LEAG VSAT priority measurement to determine the variability of volatiles distribution. The presented instrument is able to sample lunar regolith down to 10 cm, a depth at which water should be stable in certain non-permanently shadowed regions. The ability of the LVS to extract volatiles from the sample and to identify relevant species was demonstrated in a relevant environment during the characterization campaign. Its measurement capability is clearly inferior to the capabilities of competing systems, such as ESA's PROSPECT instrument package. However, with a much smaller total mass of less than

2 kg it offers an inexpensive alternative that can address many of the same scientific objectives and enable mobile in-situ prospecting for lunar volatiles.

7 Acknowledgements

The development of the LVS has been funded since 2012 through the German LUISE-2 activity by the German Aerospace Center (grant number 50JR1210) and the more recent LUVMI project funded by the European Commission as part of the Horizon 2020 framework (grant number 727220).

References

Anand, M. and Lim, S. 2014. Water in and on the Moon: recent discoveries and future prospects. *EU-Korea Conference on Science and Technology.* 2014.

Anand, M., et al. 2015. *A 'European response' to the recent Lunar Exploration and Analysis Group (LEAG) Volatiles Specific Action Team (VSAT) report on lunar volatiles.* Amsterdam : ESA's Topical Team on Exploitation of Local Planetary Materials, 2015.

Andrews, D., et al. 2015. Resource Prospector (RP) - Early Prototyping and Development. *AIAA Space Conference and Exhibition.* 2015.

Atkinson, J. and Zacny, K. 2018. Mechanical Properties of Icy Lunar Regolith: Application to ISRU on the Moon and Mars. *Earth and Space.* 2018, pp. 109-120.

Barber, S. J., et al. 2018. ProSPA: Analysis of Lunar Polar Volatiles and ISRU Demonstration on the Moon. *49th Lunar and Planetary Science Conference.* 2018.

Bussey, B., et al. 2014. *Volatiles Specific Action Team.* s.l. : Lunar Exploration Analysis Group, 2014.

Calzada-Diaz, A., Acierno, K. and Lamamy, J. 2018. ISPACE'S POLAR ICE EXPLORER: A COMMERCIAL ISRU EXPLORATION MISSION TO THESOUTH POLE OF THE MOON. *69th International Astronautical Congress .* 2018.

Carpenter, J. and Fisackerly, R. 2017. PROSPECT: ESA'S PACKAGE FOR RESOURCE OBSERVATION AND IN SITU PROSPECTING FOR EXPLORATION, COMMERCIAL EXPLOITATION AND AND TRANSPORTATION. *Lunar and Planetary Science XLVIII .* 2017.

Carrier, David W., et al. 1991. Physical Properties of the Lunar Surface. *Lunar Sourcebook - a user's guide to the moon.* s.l. : Cambridge University Press, 1991, pp. 475-594.

Clark, R. N. 2009 . Detection of Adsorbed Water and Hydroxyl on the Moon. *Science - Vol 326.* 2009 , pp. 562 - 564.

Colaprete, Anthony, et al. 2010. Detection of Water in the LCROSS Ejecta Plume. *Science.* 2010, pp. 463-468.

Creaser, C. S., West, S. K. and Wilkins, J. P. G. 200. Reactions of perfluorotri-n-butylamine fragment ions in the quadrupole ion trap: the origin of artefacts in the perfluorotri-n-butylamine calibration spectrum. *Rapid Communications in Mass Spectrometry.* 200.

Farrel, W. M., Hurley, D. M. and Zimmerman, M. I. 2015. Spillage of lunar polar crater volatiles onto adjacent terrains: The case for dynamic processes. *Geophysical Research Letters.* 2015, pp. 3160–3165.

Feistel, R. and Wagner, W. 2007. Sublimation pressure and sublimation enthalpy of H2O ice between 0 and 273.16K. *Geochimica et Cosmochimica Acta.* 2007, pp. 36-45.

Feldman, W. C., et al. 1998. Fluxes of Fast and Epithermal Neutrons from Lunar Prospector: Evidence for Water Ice at the Lunar Poles. *Science, Vol 281.* 1998, pp. 1496 -1500.

Fisher, E. A., et al. 2017. Evidence for surface water ice in the lunar polar regions using reflectance measurements from the Lunar Orbiter Laser Altimeter and temperature measurements from the Diviner Lunar Radiometer Experiment . *Icarus.* 2017.

Gancet, J., et al. 2019. LUVMI AND LUVMI-X: LUNAR VOLATILES MOBILE INSTRUMENTATION CONCEPT AND EXTENSION. *ASTRA.* 2019.

Gancet, J., et al. 2017. LUVMI: A CONCEPT OF LOW FOOTPRINT LUNAR VOLATILES MOBILE INSTRUMENTATION. *ASTRA.* 2017.

Hayne, P., et al. 2015. Evidence for exposed water ice in the Moon's south polar regions from Lunar Reconnaissance Orbiter ultraviolet albedo and temperature measurements. *Icarus.* 2015, pp. 58-69.

Hurley, Dana M., et al. 2012. Two-dimensional distribution of volatiles in the lunar regolith from space weathering simulations. *Geophysical Research Letters.* 2012.

Iai, Masafumi and Luna, Ronaldo. 2011. Direct Shear Tests on JSC-1A Lunar Regolith Simulant. *Journal of Aerospace Engineering.* 2011, pp. 433-441.

Indyk, S., Paulsen, G., et al. 2017. TRIDENT - The regolith and ice drill for exploration of new terrains. *Annual Meeting of the Lunar Exploration Analysis Group.* 2017.

Kleinhenz, J., et al. 2018. Volatiles Loss from water bearing regolith simulant at Lunar Environments. *Earth and Space.* 2018.

Li, Shuai, et al. 2018. Direct evidence of surface exposed water ice in the lunar polar regions. *Proceedings of the National Academy of Sciences.* 2018.

March, R. E. and Todd, J. F. 2005. *Quadrupole Ion Trap Mass Spectrometer.* s.l. : John Wiley & Sons Inc., 2005.

Mitrofanov, I., et al. 2012. Testing polar spots of water-rich permafrost on the Moon: LEND observations onboard LRO. *Journal of Geophysical Research: Planets, Vol 117.* 2012.

Morse, A., et al. 2015. Low CO/CO2 ratios of comet 67P measured at the Abydos landing site by the Ptolemy mass spectrometer. *Astronomy & Astrophysics.* 2015.

Nozette, S., et al. 1996. The Clementine Bistatic Radar Experiment. *Science, Vol 274.* 1996, pp. 1495--1498.

Paige, David A., et al. 2010. Diviner Lunar Radiometer Observations of Cold Traps in the Moon's South Polar Region. *Science.* 2010.

Parzinger, S., et al. 2013. Experimental Feasibility Study of On-Site Detection of OH/H2O due to In-Situ Thermal Processing of Lunar Regolith. *43rd International Conference on Environmental Systems.* 2013.

Pieters, C. M., et al. 2009. Character and Spatial Distribution of OH/H2O on the Surface of the Moon Seen by M3 on Chandrayaan-1. *Science.* 2009, pp. 568-572.

Poston, M. J., et al. 2013. Water interactions with micronized lunar surrogates JSC-1A and albite under ultra-high vacuum with application to lunar observations. *JGR Planets.* 2013, pp. 105-115.

Reiss, P. 2018. A combined model of heat and mass transfer for the in situ extraction of volatile water from lunar regolith. *Icarus.* 2018, Vol. 306.

Reiss, P., Hoehn, A. and Henn. 2015. Stamp-heater instrument concept for mobile in-situ extraction and analysis of lunar volatiles. *European Lunar Symposium.* 2015.

Robertson, I. 2016. Study of the Decomposition of Calcium Oxalate Monohydrate using a Hyphenated Thermogravimetric Analyser - FT-IR System (TG-IR). *PerkinElmer - Application Note.* 2016.

Sunshine, J. M., et al. 2009. Temporal and Spatial Variability of Lunar Hydration As Observed by the Deep Impact Spacecraft. *Science, Vol 326.* 2009, pp. 565-568.

Teodoro, L., et al. 2014. How well do we know the polar hydrogen distribution. *Journal of Geophysical Research: Planets.* 2014, pp. 574-593.

Trautner, R., et al. 2018. PROSPECT: A NOVEL PACKAGE FOR SUBSURFACE SAMPLE ACQUISITION AND ANALYSISOF LUNAR VOLATILES. *69th International Astronautical Congress.* 2018.

Wallace, W. E., P.J., Linstrom and Mallard, W.G. 2018. NIST Mass Spectrometry Data Center. *NIST Chemistry WebBook.* 2018, (retrieved September 4, 2019).

Wright, I. P., et al. 2015. CHO-bearing organic compounds at the surface of 67P/Churyumov-Gerasimenko revealed by Ptolemy. *Science.* 2015.

Zacny, K., et al. 2016. Planetary Volatiles Extractor (PVEx) for in-situ ressource utilization (ISRU) on the moon. *Annual Meeting of the Lunar Exploration Analysis Group.* 2016.

Zeng, X., et al. 2010. Geotechnical Properties of JSC-1A Lunar Soil Simulant. *Journal of Aerospace Engineering.* 2010, pp. 111-116.

Highlights:

- Regolith Sampling, Gas Extraction & Analysis Instrument for Volatiles Exploration
- Thermal-Vacuum testing of integrated instrument
- Drill testing in icy regolith simulants

Conflict of interest statement:

I hereby confirm on behalf of my co-authors and myself, that there are no conflicts of interest related to the preparation or publication of this paper. The funding sources and author affiliations are disclosed in the manuscript.

János Biswas, , Munich, 20.09.2019